ENVIRONMENTAL RESEARCH
LETTERS

PURPOSE-LED PUBLISHING™ Part of the ENVIRONMENTAL RESEARCH SERIES

LETTER • OPEN ACCESS

Adapting agriculture to climate catastrophes: the nuclear winter case

To cite this article: Yuning Shi *et al* 2025 *Environ. Res. Lett.* **20** 064006

View the article online for updates and enhancements.

You may also like

- Skilful seasonal forecasts of wind energy generation in India during the western summer monsoon
James Norman and Amanda C Maycock
- Biomass cookstove emissions—a systematic review on aerosol and particle properties of relevance for health, climate, and the environment
Natxo García-López, Ange Sabine Ingabire, Rob Bailis et al.
- Projections of climate change-attributable diarrhea burden: a systematic review
Alyssa G Miller, Molly K Miller-Petrie, River B Williams et al.



This content was downloaded from IP address 128.118.7.75 on 25/07/2025 at 19:18

ENVIRONMENTAL RESEARCH
LETTERS

LETTER

Adapting agriculture to climate catastrophes: the nuclear winter case

Yuning Shi[1], **Felipe Montes**[1], **Francesco Di Gioia**[1], **Lili Xia**[2], **Charles G Bardeen**[5], **Charles T Anderson**[3], **Yolanda Gil**[4], **Deborah Khider**[4], **Varun Ratnakar**[4] and **Armen R Kemanian**[1,*]

[1] Department of Plant Science, The Pennsylvania State University, University Park, PA 16802, United States of America
[2] Department of Environmental Sciences, Rutgers University, New Brunswick, NJ 08901, United States of America
[3] Department of Biology, The Pennsylvania State University, University Park, PA 16802, United States of America
[4] Information Sciences Institute, University of Southern California, Marina Del Rey, CA 90292, United States of America
[5] Atmospheric Chemistry Observations and Modeling Laboratory, National Center for Atmospheric Research, Boulder, CO 80307, United States of America
* Author to whom any correspondence should be addressed.

E-mail: kxa15@psu.edu

Keywords: agriculture, climate, catastrophes, modeling, food production

Supplementary material for this article is available online

OPEN ACCESS

RECEIVED
17 December 2024

REVISED
4 April 2025

ACCEPTED FOR PUBLICATION
23 April 2025

PUBLISHED
13 May 2025

Original Content from this work may be used under the terms of the Creative Commons Attribution 4.0 licence.

Any further distribution of this work must maintain attribution to the author(s) and the title of the work, journal citation and DOI.

Abstract

Following a nuclear war, destruction would extend well beyond the blast zones due to the onset of a nuclear winter that can devastate the biosphere, including agriculture. Understanding the damage magnitude and preparing for the folly of its occurrence are critical given current geopolitical tensions. We developed and applied a framework to simulate global crop production under a nuclear winter using the Cycles agroecosystem model, incorporating ultraviolet (UV)-B radiation effects on plant growth and adaptive selection of crop maturity types (shorter cycle the lower the temperature). Using maize (*Zea maize* L.) as a sentinel crop, we found that annual maize production could decline from 7% after a small-scale regional nuclear war with 5 Tg soot injection, to 80% after a global nuclear war with 150 Tg soot injection, with recovery taking from 7 to 12 years. UV-B damage would peak 6–8 years post-war and can further decrease annual maize production by 7%. Over the recovery period, adaptive selection of maize maturity types to track changing temperatures could increase production by 10% compared to a no-adaptation strategy. Seed availability may become a critical adaptation bottleneck; this and prior studies might underestimate food production declines. We propose that adaptation must include the development of Agricultural Resilience Kits consisting of region- and climate-specific seed and technology packages designed to buffer against uncertainty while supply chains recover. These kits would be congenial with the transient conditions during the recovery period, and would also be applicable to other catastrophes affecting food production.

1. Introduction

In April 1815, the eruption of Mt Tambora released sulfate aerosols that blocked solar radiation and cooled the air above the landmass by up to 2 °C, especially in the Northern Hemisphere [1]. The year 1816 became known as the 'Year without a Summer.' The socio-economic fallout of the eruption included crop failures, famines, mass human migrations, economic depressions, and famously, the downfall of Napoleon Bonaparte [2, 3]. The consequences of the Mt Tambora eruption are but a glimpse into the effects of a full-scale nuclear war on the biosphere, which would be orders of magnitude more catastrophic, with prolonged cooling, agricultural collapse, and social upheaval on an unprecedented scale. Current geopolitical tensions such as Russia's invasion of Ukraine, the simmering conflict in Kashmir, and instability in the Middle East have undermined the fragile detente that prevailed during the last years of the Cold War. Although unlikely, the risk of a nuclear war has increased, which underscores the urgent need for proactive strategies to safeguard food systems.

While a nuclear war can cause immediate and staggering death and destruction from radioactivity, fires, and direct blast effects, these represent only the

© 2025 The Author(s). Published by IOP Publishing Ltd

initial phase of the resulting global catastrophe. For instance, a regional nuclear war between India and Pakistan could cause 27 million direct deaths from the bomb blasts, while a nuclear war involving 15 countries, including the United States and Russia, could cause 360 million direct deaths [4, 5]. Longer term effects in the atmosphere following a nuclear conflict would very likely trigger a nuclear winter lasting more than a decade.

Fires and explosions from nuclear blasts release soot into the atmosphere. When soot reaches the upper troposphere or lower stratosphere, it absorbs solar radiation, heating up the surrounding air and self-lofting into the upper stratosphere [6]. Once in the upper stratosphere, the soot spreads globally, absorbing solar radiation and darkening and cooling the Earth's surface, thus triggering a nuclear winter. This abrupt climate change would shorten growing seasons, reduce solar radiation for photosynthesis, and disrupt precipitation patterns, all of which would decimate global crop production [7]. Even if supply chains and shipping lanes can be restored, global food production would still be limited.

The fallout of such anthropogenic catastrophes requires rigorous investigation to inform the public and policy decisions. Recently, combinations of climate and crop models have been used to assess the potential for regional or global food production following nuclear wars. Xia and Robock [8] modeled rice (*Oryza sativa* L.) production in 24 provinces in China, with each province represented by one model grid. Özdoğan *et al* [9] modeled maize (*Zea maize* L.) and soybean (*Glycine max* (L.) Merr.) production, with 12 $0.25^\circ \times 0.25^\circ$ grid cells centered at four locations in the Midwest United States. Jägermeyr *et al* [10] analyzed global production of maize, wheat (*Triticum aestivum* L.), rice, and soybean using six crop models with a 0.5° global grid, under the same nuclear war scenario. Xia *et al* [7] evaluated global production for the same four crops using Version 5 of the Community Land Model that includes crop growth and management (CLM5Crop) [11, 12] with a $1.9^\circ \times 2.5^\circ$ grid, under six different nuclear war scenarios, with soot injection ranging from 5 Tg to 150 Tg (1 Tg = 1 Teragram = 10^{12} g). These studies underscore the usefulness of advanced modeling techniques to predict the effects of nuclear wars on global food security. However, limitations in model assumptions and algorithms have hindered our ability to explore both the damage extent and adaptive mitigation. Among these limitations are assessing damage by ultraviolet (UV)-B radiation and adaptation through planting date adjustment and crop maturity type selection.

Stratospheric ozone (O_3) is a strong absorber of life-damaging UV radiation. The blast and fireball of atomic explosions produce nitrogen oxides (NO_x). In the stratosphere, both the presence of NO_x and heating from absorptive soot could rapidly destroy O_3 [13], increasing UV-B radiation levels at the Earth's surface. This would damage plant tissue and further limit global food production.

Adjusting planting dates and selecting appropriate crop cycles are common agronomic adaptations. Previous studies of post-catastrophic agriculture either fixed planting dates (e.g. [8, 10]) or based them on cumulative thermal time thresholds (e.g. [7, 9]). Critically, hybrids or cultivars within species were not regionally tailored to the transient climate regime of a nuclear winter. These approaches overlook dynamic human efforts to adapt to challenging conditions and the role of the rainy season onset in determining planting dates. For example, the effect of UV-B radiation increase on seed viability remains unexplored. Additionally, spatial resolutions of these studies were coarse and gridded (0.25°–2.5°), rather than tailored to geographic units of interest like provinces or countries, making it difficult for policymakers to develop targeted strategies.

The objectives of this study are to: (1) develop a framework to evaluate the impact of nuclear winters or other disruptions affecting agriculture on the global production of grain crops using maize as the sentinel crop; (2) assess UV-B radiation damage to crops by incorporating results from a controlled-conditions experiment; and (3) assess the effect on production of adaptation strategies such as the adaptive selection of maize maturity types.

In this study, we established a framework to simulate global crop production with precise planting areas, representative soil properties, and realistic planting dates. This is the first study that simulates the damage of crop growth from UV-B radiation and the potential for adaptive selection of crop maturity types. The framework is aligned with Level 3 administrative boundaries to facilitate applicability to localized policy-making and agricultural planning. Meteorological data were taken from Community Earth System Model [14] (CESM) simulated weather conditions. We used the Cycles agroecosystem model [15, 16] and simulated maize production in 38 572 locations under a control scenario and six nuclear war scenarios of increasing severity (soot injection of 5 Tg to 150 Tg). This investigation advances our understanding of global agricultural resilience and adaptation in response to catastrophic climatic disruptions.

2. Methods

2.1. Cycles agroecosystem model

Cycles [15, 16] is a multi-crop multi-year model that allows simulating plant and soil processes for

monocultures or for multi-species plant communities. Cycles has been integrated into high-performance computing workflows for large-scale high-resolution simulations [17, 18]. The model focuses on the carbon and nitrogen cycles and among its outputs is crop yield. Crops are planted on a fixed or conditional schedule. This important feature allows specifying a planting time window for each crop during which the planting will only occur if soil moisture and temperature are within preset thresholds. This ensures that planting operations are timely, enhancing the likelihood of successful crop establishment and growth. If the specified soil conditions are not met within the designated time-window, the model schedules the planting for the last day of the window, so that the agricultural cycle continues. An empirical UV-B factor was applied to reduce both the radiation-use efficiency (g biomass MJ^{-1} solar radiation) and transpiration-use efficiency (g biomass kg^{-1} water transpired) of plants growing under high UV-B radiation:

$$f_{UVB} = \frac{1}{1 + \left(\frac{UVB}{16}\right)^4}, \quad (1)$$

where UVB is in the unit of kJ m^{-2} d^{-1}. This equation was based on a greenhouse experiment on wheat and assumed to apply to all crops until more information becomes available. In the experiment, wheat exposed to 15 kJ m^{-2} d^{-1} decreased biomass production by 40% compared with the control, without a reduction in the proportional partitioning of biomass to grain. Accordingly, the equation states that under 16 kJ m^{-2} d^{-1} of UV-B, daily growth is reduced by 50% compared to optimum conditions. The power of 4 affects the steepness of the response and ensures that the damage starts after UV-B exceeds 6 kJ m^{-2} d^{-1}, the sea-level daytime UV-B on a sunny summer day.

2.2. Data

To facilitate global high-resolution agroecosystem simulations using the cycles model, we built a cycles global simulation database that is aligned with current Level 3 administrative boundaries. The EarthStat Harvested Area and Yield for 175 Crops database [19], the updated Global Agro-Ecological Zones 2015 dataset version 4 [20], and the European Space Agency Climate Change Initiative Land Cover 2015 land cover map [21] were combined to capture the rainfed and irrigated harvested areas of crops in different regions. Soil physical parameters were obtained from the SoilGrids database [22]. We also assigned the corresponding Global Land Data Assimilation System [23] grid to each region and created Cycles weather files for all grids that contain cropland. The result is the Cycles global simulation database that supports the simulations of major crops in any Level 3 (e.g. county) administrative region in the world.

Table 1. Stratospheric soot injection for a control scenario and six nuclear bomb exchange scenarios.

Soot injection (Tg)	Involved nations	UV-B data
0 (control)	N/A	Available
5	India, Pakistan	Available
16	India, Pakistan	N/A
27	India, Pakistan	N/A
37	India, Pakistan	N/A
47	India, Pakistan	N/A
150	US, Russia	Available

An algorithm to determine the planting dates of maize for any given region was developed following [24]'s examination of the global planting date patterns for maize and wheat. For details of the Cycles global simulation database and planting date algorithm, please refer to the Supplementary Data.

For the simulations, we considered 10 putative maize maturity types from relative maturity group 70 (RM70) to group 115 (RM115), which, considering a base temperature of 6 °C, we interpreted as requiring thermal times to maturity that vary from 1300 to 2425 growing °C days. For each location, the maize maturity group corresponds to that whose required thermal time to maturity is the closest to 0.85×thermal time of the location.

Six nuclear war scenarios with varying soot injections and a control scenario (table 1) were simulated, driven by the CESM simulated global meteorological conditions [7], with the Whole Atmosphere Community Climate Model version 4 for its atmospheric component, the Community Land Model 4.0 as the land surface model, and the Parallel Ocean Program v2 as the ocean model. Soot transport and removal in CESM is simulated using the Community Aerosol and Radiation Model for Atmospheres , in which soot is treated as fractal particles. The size of particles can change through coagulation and sedimentation and removed through gravitation or precipitation. For the India–Pakistan war scenarios, the soot was injected above individual targeted urban regions. For the global war scenario, soot was injected uniformly over the areas of Russia and the United States. In all scenarios, the soot injection lasts about a week, after the initial disruption on May 15. The spread of soot in the stratosphere, however, is rapid, and can engulf the hemisphere in days or weeks. Thus, the simulation results are not sensitive to the exact locations of soot injection. The control scenario had 19 simulation years, with each simulation year resembling the Year 2000 conditions with some perturbations. The simulated 3 h meteorological conditions were aggregated to daily temporal resolution to drive offline Cycles simulations. For details of the CESM simulations refer to [25, 26].

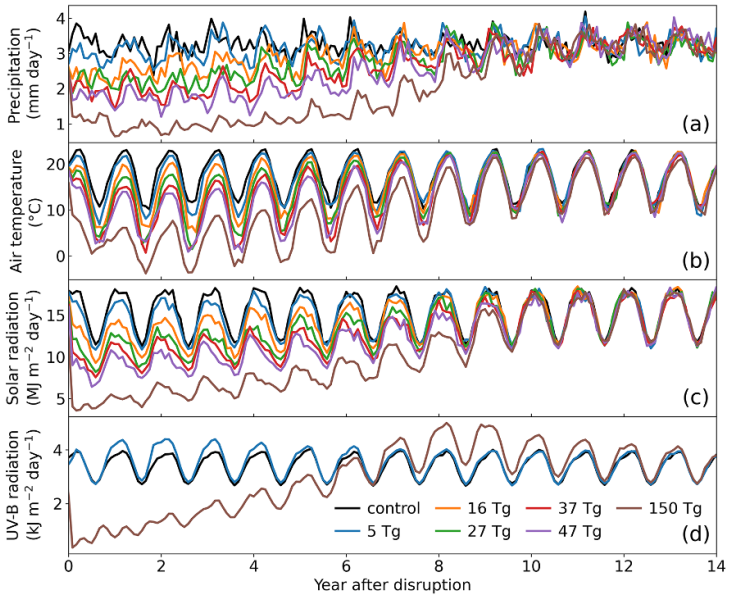


Figure 1. Monthly key meteorological variables averaged over global maize areas after disruption, under different soot injection scenarios, including (a) precipitation, (b) air temperature, (c) total solar radiation, and (d) UV-B radiation. In (d) only the control, 5 Tg, and 150 Tg data are shown. The year is defined from 15 May (starting date of soot injection) to 14 May of the following year. Precipitation and solar radiation decrease by as much as 70% globally, and air temperature drops by over 15 °C in the 150 Tg scenario. UV-B radiation load at sea level depends on both O_3 depletion caused by stratosphere heating and shielding from the soot.

Bardeen *et al* [27] simulated monthly clear-sky UV radiation with the CESM under three scenarios: the control, 5 Tg, and 150 Tg scenarios. To obtain the surface UV-B radiation with cloud cover, we assessed the simulated clear-sky UV-B radiation from the control simulation with the observed UV-B radiation at six SURFRAD [28] (surface radiation budget observing network) stations in Year 2000 to derive a rescaling factor. The rescaling factor was applied globally to all simulations to calculate the monthly surface UV-B radiation with cloud cover from [27] monthly clear-sky UV-B radiation and then interpolated to daily values assuming the daily UV-B radiation changes proportionally with daily downward solar radiation.

2.3. Experiment design

We conducted simulations of rainfed maize production across all Level 3 administrative regions, focusing on areas where rainfed maize was harvested as per data from the Cycles global simulation database. Each simulation assumed a single annual planting, and the model operated under conditions of no stress from nutrients, weeds, or pests.

We used the control scenario multi-year average meteorological condition and our planting date algorithm to calculate a reference planting date for each region. For all simulations, the planting window was set to be 98 d, beginning 7 d before the reference date, and extending 90 d after the reference date. The multi-year average meteorological condition was also used to calculate the average thermal time, which determined a default maturity type for each region.

For the control scenario, the default maturity type was planted every year. Cycles simulation results from the control scenarios were averaged across years to obtain a reference background free of interannual perturbations. The six nuclear war scenarios were run both with and without maturity type adaptation. Without maturity type adaptation, the default maturity type was planted every year, as in the control scenario. With adaptation, the default maturity type was planted in the year of and prior to the disruption; but in the post-disruption years, the choice of maturity type was determined by the thermal time of the corresponding year, simulating optimal adaptation capacity. This approach presumes that seed for each maturity type for each region is available. Under the circumstances of a nuclear winter this is overly optimistic but provides an estimation of the maize production upper bound under the transient conditions of nuclear winters.

For the three scenarios that had UV-B data (table 1), the adaptation simulations were also run with and without the UV-B forcing, i.e. with and without UV-B stress.

3. Results

3.1. Transient climatic conditions post disruption

After soot injection, precipitation, air temperature, and solar radiation decreased immediately compared to the control scenario, making maize harvested areas drier, colder, and darker (figure 1). The meteorological variables were averaged for the global rainfed maize areas, and since the Northern Hemisphere

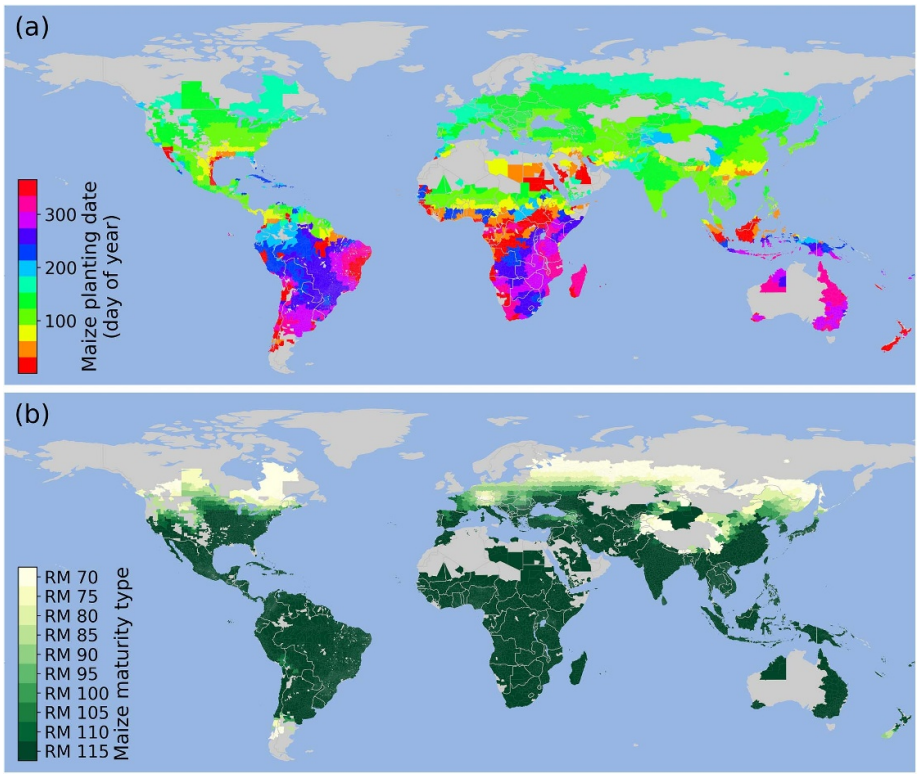


Figure 2. Maps of predicted (a) planting dates and (b) maturity types for the control scenario in each level 3 administrative region.

has more area dedicated to maize, the spatially averaged variables are biased showing higher air temperature and solar radiation in the northern summer. The extent and duration of these effects relate to the amount of soot injected. For the most devastating 150 Tg scenario, precipitation and solar radiation decrease by as much as 70% globally, and air temperature drops by over 15 °C a few years after the disruption. Soot in the stratosphere absorbs solar radiation and heats the stratosphere helping deplete O_3. Simultaneously, soot absorbs UV-B radiation thus shielding the surface from exposure. In the 5 Tg regional war scenario, the shielding effect of soot dominates soon after the war, reducing UV-B radiation. About one year later, the depletion of O_3 and the deposition of the soot allow UV-B radiation to reach the Earth surface at levels above those of the control scenario. UV-B radiation returns to pre-disruption levels after six years. In contrast, in the 150 Tg global war scenario, UV-B radiation initially decreases significantly due to soot absorption, but after six years, UV-B radiation levels surpass the control as soot decreases and the depleted O_3 allows the transmission of UV-B radiation. The UV-B levels would peak in Years 8 and 9.

3.2. Planting dates and maturity types

The predicted planting dates and RM types of maize under control conditions (figure 2) align closely with observations as shown in [24] (their figure 2(a)) and [29] (their figure 4.1). In mid-latitude regions of the Northern Hemisphere, planting is temperature-limited, with dates typically falling between April and May and showing a latitudinal gradient. In tropical and southern mid-latitude regions, planting is more variable due to precipitation-limited regimes, with spatial patterns reflecting the timing of rainy seasons. Figure 2(b) shows the calculated default maturity types. Longer season maturity types are planted in the neotropics and southern mid-latitudes. Analogously, maturity types exhibit a latitudinal gradient in the mid-latitude areas of the Northern Hemisphere.

3.3. Global maize production drops post disruption

The impact of soot injection on maize production is more pronounced in the Northern Hemisphere and more acute at higher latitudes (figures 3, 4 and 5(a)). In the 5 Tg scenario, maize production decreases predominantly in the Middle East, Central Asia, and Siberia and the conflict zone of India and Pakistan. Major maize-producing regions, such as the Corn Belt in the United States, southern Brazil, and northeastern China, remain largely unaffected. Consequently, global maize production is minimally affected. However, when soot injection reaches 16 Tg, adverse effects extend to major maize-producing regions including the U.S. Corn Belt and China (figure 4). Maize production in the Southern Hemisphere is mostly unscathed in both the 5 Tg and 16 Tg scenarios.

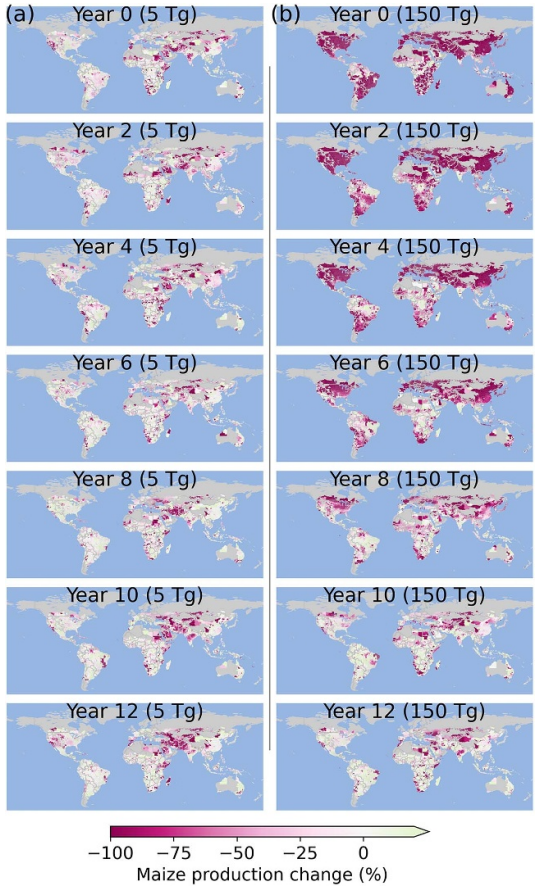


Figure 3. Relative changes of global rainfed maize production by year using a planting date and maturity type adaptation strategy for the (a) 5 Tg scenario and (b) 150 Tg scenario, compared to the control. Damage of the 5 Tg scenario is mostly on the Northern Hemisphere, but the 150 Tg scenario demolishes maize production globally.

In the most devastating global war scenario, maize production plummets to near zero except in the tropics (figure 5(a)). The effect of soot injection can last over a decade across all scenarios but is the strongest in the first four years after disruption. Maize production decreases as soot injection increases. Reductions can be as large as 9% (5 Tg), 27% (16 Tg), 44% (27 Tg), 55% (37 Tg), 60% (47 Tg), and 80% (150 Tg) compared with the control over the four years after the disruption with adaptation strategy applied (figures 6(a) and (c)).

The recovery rate of global maize production negatively correlates with the amount of soot injection. The running average of annual relative production indicates that it takes 7, 8, 11, 12, 11, and 12 years, respectively, for the global total maize production to recover to 95% of the control scenario level. Production in the Southern Hemisphere recovers faster than the Northern Hemisphere, and production at lower latitudes recovers faster than at higher latitudes.

The global maize harvested area decreases by 2% (5 Tg), 9% (16 Tg), 23% (27 Tg), 38% (37 Tg), 49% (47 Tg), and 70% (150 Tg). Maize harvested areas remained within 95% of the control level in the 5 Tg and 16 Tg scenarios, whereas in the more severe scenarios recovery takes between 5 years (27 Tg) and 10 years (150 Tg).

3.4. Benefit of adaptive selection of maize maturity types

Over the 13 years after the disruption, adaptive selection of maturity types to match the newly existing climate conditions can increase total maize production from 1.1% (5 Tg) to 10% (150 Tg), with a progressively more important effect as the soot injection level increases (figures 6(a) and (b)). For the 5 and 16 Tg scenarios, the adaptation strategy is most effective in relative terms one year post disruption, while for the 37 and 47 Tg scenarios it is most effective five and six years post disruption, respectively, and for the 150 Tg scenario it is most effective two years post disruption. The global maize harvested area with adaptive selection of maturity types compared with the default shows the same pattern as the change in maize production (figures 6(c) and (d)).

3.5. Damage from UV-B radiation would diminish crop yields after a nuclear war

The effect of UV-B radiation on total global maize production under the 5 Tg scenario is about the same level as the control scenario (figure 6(e)), despite an increase in UV-B radiation, especially in the first six years post-disruption (figure 1(d)). For the 150 Tg scenario, the net effect of UV-B on maize production is smaller than under the control scenario in the first five years post-disruption. Thereafter, damage to maize production intensifies and is strongest in Year 8 (−7.4%), recovering to background level thereafter (figures 6(e) and (f)).

3.6. Changes in seed demand

Because of the adaptive selection of maize maturity types, the global maize seed demand changes over time and across scenarios (figure 5(b)). The total seed demand is the lowest in year 0 and recovers to background levels gradually. Compared to the control scenario, however, there is increased demand of short season maize (RM < 80) and a decrease in demand of the longer maturity types due to the shortening of the growing seasons (figure 5(b)). The demand of the short-cycle types progressively increases in the first years following the nuclear conflict.

4. Discussion

An all-out nuclear war and subsequent nuclear winter would be devastating for humanity and the biosphere. This includes the effect on crop production, represented in our study by maize, which is the most widely

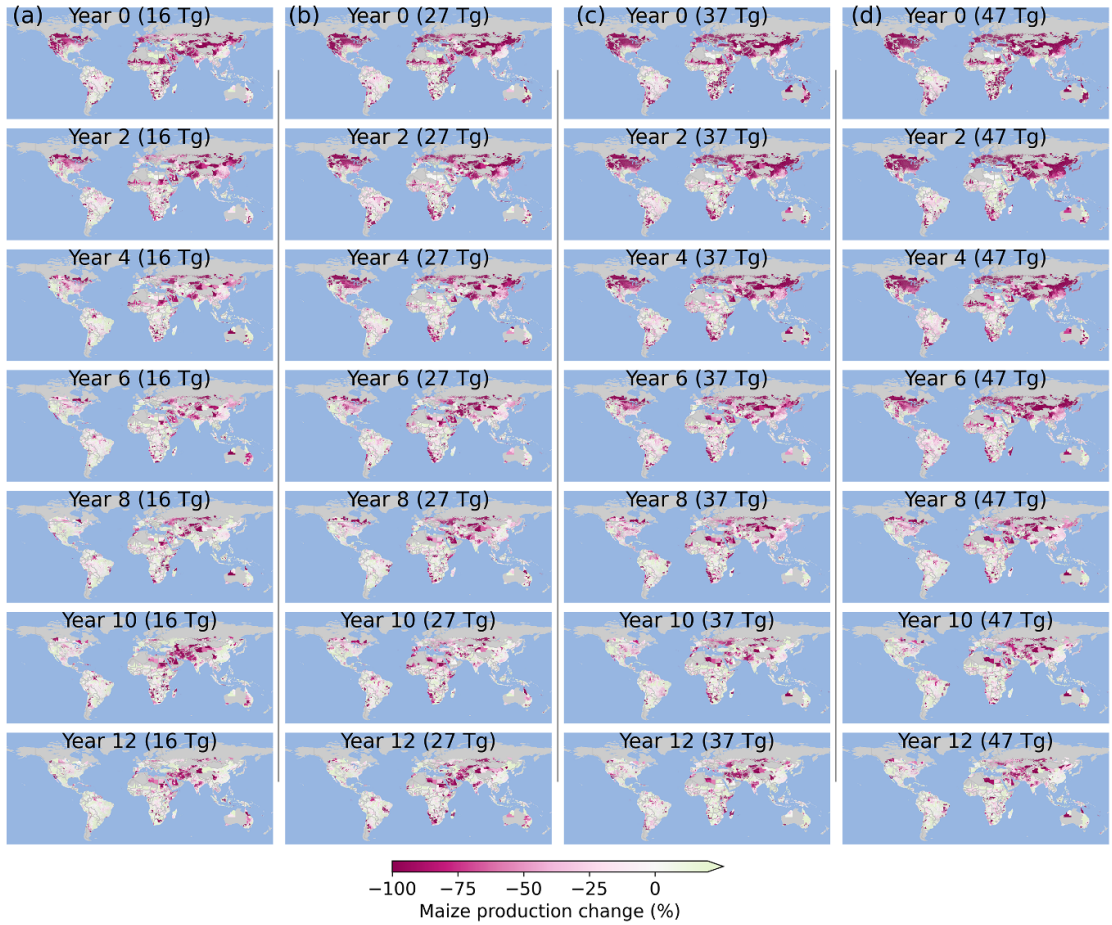


Figure 4. Relative changes of global rainfed maize production by year using a planting date and maturity type adaptation strategy for the (a) 16 Tg, (b) 27 Tg, (c) 37 Tg, and (d) 47 Tg scenarios, compared to the control scenario. Impact of nuclear winters worsens with the increase of soot injection.

planted grain crop in the world. Although only a small fraction of maize production is used for direct human consumption, its production is representative of total grain crop production and global agriculture. While earlier studies have explored the effect of nuclear conflict on climate and food production relying on the same climatic database [7], this is the first study that simulates both the additional damage derived from UV-B radiation and the potential for agricultural adaptations to partially ameliorate the crop losses resulting from soot injection in the stratosphere.

Some qualifications are needed before discussing the results. First, the simulations were driven by weather conditions predicted by the CESM. The accuracy of the assessment is partly dependent on the accuracy of the CESM simulations. Second, the control scenario represents production without agronomic limitations and overestimates production in regions with large yield gaps like those in sub-Saharan Africa [30, 31]. Nonetheless, this study focuses on relative production changes, and these are relevant despite regional differences in agricultural technology use. While regions with low productivity contribute marginally to global total production and their overestimation does not significantly affect our overall conclusions, the relative reduction is of local relevance. In addition, Cycles is a process-based agroecosystem model that accounts for key biophysical and physiological processes that determine crop growth. The model allows us to capture the response of crops to stressors dynamically rather than relying solely on empirical relationships that may be more sensitive to input biases. While absolute yield projections could indeed be influenced by uncertainties in climate forcing, the comparative trends observed across scenarios remain robust. Lastly, these catastrophic decreases in production may still underestimate the magnitude of the damage of nuclear winters. We assumed both functional markets and supply chains for seed and other inputs production and distribution. The assumptions become less tenable the more severe the nuclear conflict. In extreme cases, the human population would be not only decimated but technologically impaired. Assessments like those of [7] likely underestimate the severity of societal and

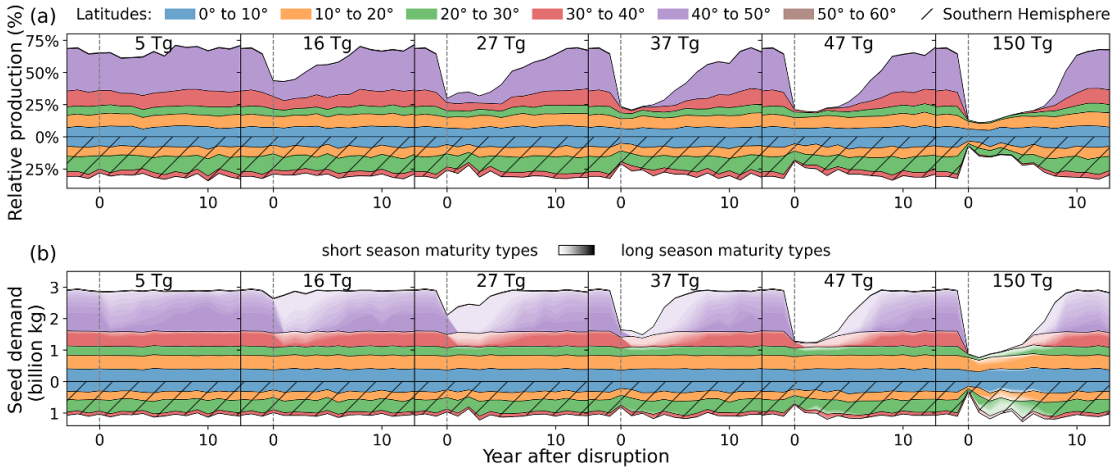


Figure 5. For each scenario, (a) global annual rainfed maize production at different latitudes relative to the control, and (b) seed demand for each maize maturity type under each scenario, assuming a seeding rate of 40 kg ha^{-1}. Colors represent different latitudes; hashed and un-hashed areas represent the Southern and Northern Hemisphere, respectively. The color gradients in (b) represent maize maturity groups, with lighter colors indicating short and darker colors long season maturity types. Impact of nuclear winters is stronger in the Northern Hemisphere than in the Southern Hemisphere, and stronger at higher latitudes compared with the neotropics. Compared to the control scenario, nuclear winters increase the demand for short season maize maturity types.

technological collapses compounding the damage of nuclear winter.

Only rainfed maize was simulated in this study. The drop of irrigated maize production could be more significant, because the decrease in precipitation (figure 1(a)) could make production of irrigated maize, and other crops, even more challenging.

The Northern Hemisphere, with its larger land mass and maize production, is more severely affected than the Southern Hemisphere, because the latter is mostly covered by oceans and cooling is stronger over land than over ocean. Moreover, the landmass in the Southern Hemisphere is concentrated closer to the equator, which experiences less cooling than higher latitudes (figure SM1). Such effects were also reported by [32–34] when studying the aftermath of volcano eruptions. However, the CESM may underestimate the cooling of Southern Hemisphere oceans, because of its known warm biases in southern-ocean surface temperature predictions [35–37], and may lead to overestimations of maize production in the Southern Hemisphere. A sensitivity analysis would provide additional insights into the potential errors introduced by biases in climate forcing.

The reduction of global maize production under different scenarios predicted using our modeling framework agrees with similar studies (e.g. [7], figure SM2), and builds on earlier work by considering the UV-B effect and adaptation strategies, such as adjusting planting dates and selecting appropriate maturity types. Dynamic selection of maize maturity type can improve production over the 13 year post-disruption period by 10% for the global war scenario. This estimate of adaptation is, however, overly optimistic, because the adaptation approach presumes that seed for each maturity type (i.e. hybrid) for each region is available and also requires prior knowledge of the weather of coming years, although the prior year can be a safe surrogate. Applying these strategies can be the difference between harvesting edible grain and regional famine. These are not purely hypothetical scenarios; the Mt Tambora eruption caused famines in the Northern Hemisphere with severe cold extending to southern China [38]. It also needs to be noted that our estimate of UV-B impact on crop growth was based on a greenhouse experiment on wheat. Although the photosynthetic apparatus is conserved in plants, different crop species may exhibit varying sensitivities to UV-B radiation due to differences in leaf structure, protective mechanisms, and physiological responses. Future research incorporating crop-specific UV-B response data would further refine these estimates.

Although not reported here, experiments conducted in controlled environments indicate that plants growing under high UV-B load (e.g. 15 kJ m^{-2} d^{-1}), although damaged, produce viable seed (Di Gioia and Kemanian, personal communication). This is a critical finding, because although seed availability is not secured in a nuclear winter scenario, seed production is still feasible. Still, in the most severe scenarios, the demand for short-season maize seed would increase by several-fold compared with current seed demand (figure 5(b)), while seed production and distribution could be severely limited. Hybrid seed production depends on a sophisticated supply chain that maintains genetically pure lines that are hybridized and harvested for seed in specific locations around

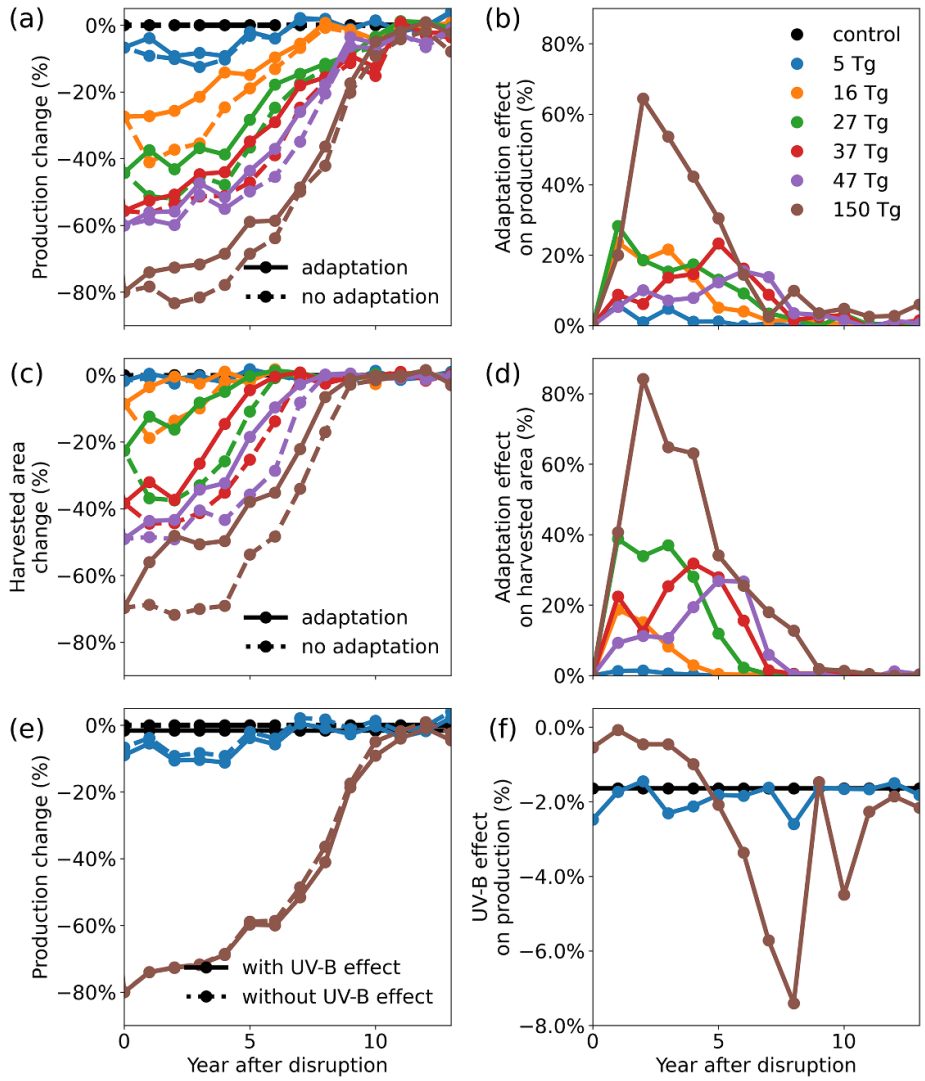


Figure 6. Global annual total rainfed maize production under different scenarios: (a) with and without adaptation strategy relative to the control scenario, and (b) with a relative representation of the effect of adaptation strategy on global maize production. Panels (c) and (d) are analogous but for the effect of adaptation on global maize harvested area; panels (e) and (f) are also analogous, but for the effect of UV-B on global rainfed maize production. Annual maize production could decline from 7% (5 Tg scenario) to 80% (150 Tg scenario), with recovery taking from 7 to 12 years. UV-B damage can further decrease annual maize production.

the world. A substantial portion of this network is in the Northern Hemisphere. If this supply chain were severely disrupted, it is likely that for many years, production of open pollinated annual crops like maize or sunflower would rely on local populations [39] or populations that are quickly developed with the seed at hand. Such seed will render crops locally non-adapted and yielding well below potential for years.

Producers can switch to other crops, although that is not always possible at scale due to seed, agrochemical, and machinery requirements. Yet, a quick shift to cool season crops like wheat, barley or potatoes at mid latitudes could be necessary under post-catastrophic conditions [39]. Such a shift would require careful planning, particularly pertaining to seed availability. An Agricultural Resilience Kit (ARK) tailored for a shifting climate could be a critical tool for maintaining food security after a catastrophe of the magnitude of a nuclear conflict. Such a kit would contain a region- and climate-tailored mix of seed that can be strategically distributed to buffer against uncertainty while supply chains recover, crop-tailored information on cultural techniques, and a model-based decision support tool to explore options since historical records and local experience become less relevant. Genetic resources studies [39, 40] and seed sources such as the USDA Germplasm Resources Information Network [41] can aid in the design of ARKs. In the long-term, such seeds would preserve crop genetic diversity. Nonetheless, the more severe the nuclear war, the deeper the reversion to primitive forms of production as the production ecosystem degrades.

The successful deployment of ARKs would require pre-disaster preparedness and adaptive management. The ARKs should be developed and

positioned in key agricultural regions; distributed through coordinated global, national, and regional efforts in the event of a crisis; and continuously evaluated and adjusted to ensure accessibility in times of crisis. The maintenance and administration of ARKs would require therefore collaboration among nations.

Beyond nuclear winter, specialized or geographically concentrated agriculture is vulnerable to extreme climate events. For example, Iowa, a state representative of the US Midwest, has about 2/3 of its area under maize or soybean [42]. Heat domes and heat stress [43, 44], or cold snaps, can devastate crops in such regions. This study underscores not just the risk of nuclear conflict, but the broader vulnerability of agricultural production to extreme climate disruptions. Addressing these risks and vulnerabilities requires predictive tools like those presented in this study, and a strategy for adapting agriculture to severe climate events. Our society is currently poorly prepared for global catastrophic events, but this is a solvable condition.

5. Conclusions

Nuclear wars would cause an unfathomable loss of life and genetic resources, but also a prolonged nuclear winter that would reduce agricultural area and productivity for years. A severe disruption of supply chains and commerce can aggravate this loss of productivity, leading to regional or global famines. As the climate recovers, high UV-B radiation could further damage crops, with effects manifesting years after the nuclear conflict. Proactive measures must be taken to mitigate its potential impacts on global food security. This requires strategic investment in ARKs, international collaboration on agricultural resilience planning, and the integration of nuclear winter scenarios into broader climate adaptation policies. This study shows that adaptation strategies like dynamic tailoring of maize maturity types can improve food production by 10% over a 13 year recovery period compared with static approaches under a global nuclear war scenario. That is a lot of lives saved. Simulation models and tools such as those presented in this study can aid in planning such adaptive strategies. These preparations can increase our resilience to other catastrophic events, such as volcanic eruptions, extreme climate events, or pest outbreaks that threaten food production. Yet, when it comes to a nuclear winter, the best approach to preventing its devastating effects is to avoid it.

Data availability statement

The data that support the findings of this study are openly available at the following URL/DOI: https://doi.org/10.5281/zenodo.15113980.

Acknowledgments

This research was supported by Open Philanthropy, and the Defense Advanced Research Projects Agency under Award W911NF-18-1-0027. Y S and A R K were in addition supported by the USDA National Institute of Food and Agriculture Federal Appropriations under Project #PEN05016, Accession #7007513, and Project #PEN05001, Accession #7007612, respectively. L X was supported by the US National Science Foundation (Grant No. AGS-2017113) and by the Future of Life Institute.

ORCID iDs

Yuning Shi https://orcid.org/0000-0003-0118-5847
Felipe Montes https://orcid.org/0000-0003-1113-6969
Francesco Di Gioia https://orcid.org/0000-0003-3509-3190
Charles G Bardeen https://orcid.org/0000-0002-5330-2788
Charles T Anderson https://orcid.org/0000-0001-7481-3571
Yolanda Gil https://orcid.org/0000-0001-8465-8341
Deborah Khider https://orcid.org/0000-0001-7501-8430
Varun Ratnakar https://orcid.org/0000-0001-9381-705X
Armen R Kemanian https://orcid.org/0000-0002-7682-3527

References

[1] Kandlbauer J, Hopcroft P O, Valdes P J and Sparks R S 2013 *J. Geophys. Res.: Atmos.* **118** 12497–507
[2] Wheeler D and Demarée G 2005 *Weather* **60** 159–64
[3] Genge M J 2018 *Geology* **46** 835–8
[4] Toon O B, Turco R P, Robock A, Bardeen C, Oman L and Stenchikov G L 2007 *Atmos. Chem. Phys.* **7** 1973–2002
[5] Toon O B, Robock A and Turco R P 2008 *Phys. Today* **61** 37–42
[6] Ohneiser K, Ansmann A, Witthuhn J, Deneke H, Chudnovsky A, Walter G and Senf F 2023 *Atmos. Chem. Phys.* **23** 2901–25
[7] Xia L, Robock A, Scherrer K, Harrison C S, Bodirsky B L, Weindl I, Jägermeyr J, Bardeen C G, Toon O B and Heneghan R 2022 *Nat. Food* **3** 586–96
[8] Xia L and Robock A 2013 *Clim. Change* **116** 357–72
[9] Özdoğan M, Robock A and Kucharik C J 2013 *Clim. Change* **116** 373–87
[10] Jägermeyr J *et al* 2020 *Proc. Natl Acad. Sci.* **117** 7071–81
[11] Lawrence D M *et al* 2019 *J. Adv. Model. Earth Syst.* **11** 4245–87
[12] Lombardozzi D L, Lu Y, Lawrence P J, Lawrence D M, Swenson S, Oleson K W, Wieder W R and Ainsworth E A 2020 *J. Geophys. Res.: Biogeosci.* **125** 1–19
[13] Mills M J, Toon O B, Turco R P, Kinnison D E and Garcia R R 2008 *Proc. Natl Acad. Sci.* **105** 5307–12
[14] Hurrell J W *et al* 2013 *Bull. Am. Meteorol. Soc.* **94** 1339–60

[15] Shi Y, Montes F and Kemanian A R 2023 *Water Resour. Res.* **59** e2022WR033453
[16] Kemanian A R, Shi Y, White C M, Montes F, Stöckle C O, Huggins D R, Laura Cangiano M, Stefani-Faé G and Nydegger Rozum R K 2024 *Comput. Electron. Agric.* **227** 109510
[17] Silva R F D, Mayani R, Shi Y, Kemanian A R, Rynge M and Deelman E 2019 *Proc.—2019 IEEE Int. Conf. on Big Data, Big Data 2019* pp 4545–52 (available at: https://ieeexplore.ieee.org/abstract/document/9006107)
[18] Gil Y *et al* 2021 *ACM Trans. Interact. Intell. Syst.* **11** 1–49
[19] Monfreda C, Ramankutty N and Foley J A 2008 *Glob. Biogeochem. Cycles* **22** 1–19
[20] Grogan D, Frolking S, Wisser D, Prusevich A and Glidden S 2022 *Sci. Data* **9** 1–16
[21] Bontemps S *et al* 2015 Multi-year global land cover mapping at 300 M and characterization for climate modelling: achievements of the land cover component of the ESA climate change initiative *International Archives of the Photogrammetry, Remote Sensing and Spatial Information Sciences—ISPRS Archives* vol 40 (International Society for Photogrammetry and Remote Sensing) pp 323–8
[22] Poggio L, De Sousa L M, Batjes N H, Heuvelink G B, Kempen B, Ribeiro E and Rossiter D 2021 *Soil* **7** 217–40
[23] Rodell M *et al* 2004 *Bull. Am. Meteorol. Soc.* **85** 381–94
[24] Sacks W J, Deryng D, Foley J A and Ramankutty N 2010 *Glob. Ecol. Biogeogr.* **19** 607–20
[25] Coupe J, Bardeen C G, Robock A and Toon O B 2019 *J. Geophys. Res.: Atmos.* **124** 8522–43
[26] Toon O B, Bardeen C G, Robock A, Xia L, Kristensen H, McKinzie M, Peterson R J, Harrison C S, Lovenduski N S and Turco R P 2019 *Sci. Adv.* **5** 1–14
[27] Bardeen C G *et al* 2021 *J. Geophys. Res.: Atmos.* **126** 1–22
[28] Augustine J A, DeLuisi J J and Long C N 2000 *Bull. Am. Meteorol. Soc.* **81** 2341–57
[29] Bansal S and Nagarajan M 2022 Portfolio management issues in the commercial seed industry: a modeling framework and industry implementation *Agricultural Supply Chain Management Research* (Springer) pp 53–67
[30] van Ittersum M K, Cassman K G, Grassini P, Wolf J, Tittonell P and Hochman Z 2013 *Field Crops Res.* **143** 4–17
[31] Hoffman A L, Kemanian A R and Forest C E 2018 *Glob. Change Biol.* **24** 143–57
[32] Hansen J, Lacis A, Ruedy R and Sato M 1992 *Geophys. Res. Lett.* **19** 215–8
[33] Raible C C *et al* 2016 *Wiley Interdiscip. Rev.-Clim. Change* **7** 569–89
[34] Wilson N, Valler V, Cassidy M, Boyd M, Mani L and Brönnimann S 2023 *Sci. Rep.* **13** 3649
[35] Kang S M, Ceppi P, Yu Y and Kang I S 2023 *Nat. Geosci.* **16** 775–80
[36] Ma J, Xu S and Wang B 2019 *Ocean Dyn.* **69** 939–54
[37] Kay J E, Wall C, Yettella V, Medeiros B, Hannay C, Caldwell P and Bitz C 2016 *J. Clim.* **29** 4617–36
[38] Gao C, Gao Y, Zhang Q and Shi C 2017 *J. Meteorol. Res.* **31** 28–38
[39] McLaughlin C M, Shi Y, Viswanathan V, Sawers R J H, Kemanian A R and Lasky J R 2025 *Nat. Commun.* accepted
[40] FAO 2025 The third report on the state of the world's plant genetic resources for food and agriculture *Technical Report* (Food and Agriculture Organization of the United Nations)
[41] Wiersema J H 1995 *Acta Hortic.* **413** 109–16
[42] U.S. Department of Agriculture, National Agricultural Statistics Service 2024 2022 census of agriculture *Technical Report* (U.S. Department of Agriculture)
[43] Schlenker W and Roberts M J 2009 *Proc. Natl Acad. Sci.* **106** 15594–8
[44] Hoffman A L, Kemanian A R and Forest C E 2020 *Environ. Res. Lett.* **15** 094013